



## On the Dependence of the Surface Roughness of Electrochemically Anodized Silicon on Ion Irradiation Fluence

S. Azimi,<sup>z</sup> Y. S. Ow, and M. B. H. Breese

Physics Department, National University of Singapore, 119260 Singapore

We have studied the dependence of the surface roughness of electrochemically anodized p-type silicon on ion irradiation fluence. For moderate resistivity wafers, the surface roughness reduces with fluence, consistent with the dominant effect being a reduced anodization rate. However, for low resistivity wafers, the surface roughness increases with fluence. This is explained by showing how irradiation converts the low wafer resistivity, which tends to form mesoporous silicon with low associated roughness, into a moderate resistivity, which tends to form microporous silicon with high associated roughness. This result explains why the anomalous behavior of surface roughness and photoluminescence intensity is observed.  
© 2010 The Electrochemical Society. [DOI: 10.1149/1.3481769] All rights reserved.

Manuscript submitted June 28, 2010; revised manuscript received August 2, 2010. Published August 31, 2010.

A process for silicon micromachining based on a combination of high energy ion beam irradiation and electrochemical anodization was recently developed.<sup>1-6</sup> MeV ions, typically protons or helium ions, are used to irradiate p-type silicon wafers, which results in a localized increase in their resistivity by creating point defects along the ion trajectories.<sup>1,7</sup> The increased resistivity of the irradiated silicon locally reduces the current flowing through these regions during subsequent electrochemical anodization,<sup>1</sup> so the rate of formation of porous silicon slows down or may be completely stopped for high fluences. The underlying micropatterned silicon surface may then be revealed by removing the PSI with potassium hydroxide (KOH).

Many types of patterned porous silicon and silicon surface structures have been fabricated using this process, such as patterned distributed Bragg reflectors,<sup>8</sup> microturbines<sup>2</sup> and waveguides,<sup>9</sup> and variable photoluminescence (PL) wavelength and intensity.<sup>6,10</sup> Many applications require as smooth a surface as possible,<sup>11</sup> such as low loss silicon photonic components, so it is important to study the underlying causes of surface roughness. Different applications typically use differing resistivity silicon as the starting material. For example, silicon photonic devices normally use moderate or high resistivity wafers of more than 1  $\Omega$  cm to minimize optical losses due to free carrier scattering, whereas low resistivity wafers of less than 0.1  $\Omega$  cm are preferred for micromachining surface relief patterns with multiheight steps, micromirrors, and holographic surfaces, because it is easier to machine a range of differing step heights. Hence, it is important to know how each different resistivity behaves as a function of ion irradiation fluence.

We have previously compared the surface roughness resulting from the use of ion irradiation as a means of patterning and machining silicon surfaces<sup>12</sup> using two methods of MeV ion irradiation: first, direct-write irradiation using a scanned, focused beam, and second, large area irradiation using a large beam current incident on the wafer through a thick, patterned photoresist on the surface. The large area method resulted in significantly smoother surfaces at the irradiated regions because of the high lateral uniformity of irradiation compared with direct writing, where variations in the focused beam current can strongly increase the surface roughness by causing nonuniformities of the irradiation.

The mechanism by which silicon undergoes dissolution during electrochemical anodization depends on the wafer doping density. For moderate resistivity wafers (0.1–10  $\Omega$  cm), thermionic emission within the space charge region, together with quantum confinement effects, results in microporous silicon formation. For low resistivity wafers of less than 0.1  $\Omega$  cm, tunneling effects occur across the space charge region, leading to the formation of mesoporous silicon.

Other factors can influence the surface roughness of the anodized wafers, such as anodized layer thickness and anodization current

density. All these factors were studied by Lerondel et al.<sup>13</sup> Moderate resistivity wafers produce anodized surfaces with high roughness. The roughness increases linearly with layer thickness up to  $\sim 1$   $\mu\text{m}$ , where the roughness reaches a value of 10–20 nm. For thicker anodized layers, the roughness saturates at 20–40 nm. Low resistivity wafers produce anodized surfaces with low roughness. The roughness exhibits a much weaker dependence on layer thickness, with values of only a few nanometers obtained for anodized layers thicker than 10  $\mu\text{m}$ . For a low anodization current density ( $j < 50$  mA/cm<sup>2</sup>), the roughness rapidly increases with decreasing  $j$ . At a high current density ( $j > 100$  mA/cm<sup>2</sup>), the roughness is independent of  $j$ .

Here, the effects of ion irradiation on the anodized surface roughness of three p-type wafer resistivities of 0.02, 0.5, and 5  $\Omega$  cm were studied. Figure 1 shows a schematic of the effect of ion irradiation on the subsequent anodization process. After irradiation (Fig. 1a), the increased resistivity of the irradiated region reduces the hole current density flowing through it during subsequent anodization (Fig. 1b); the size of reduction depends on the fluence. Wafers were anodized in an electrolyte containing HF (48%):water:ethanol in the ratio of 1:1:2 for 130, 180, and 180 s, respectively. The thickness of the PSI is taken to be the height difference between the irradiated

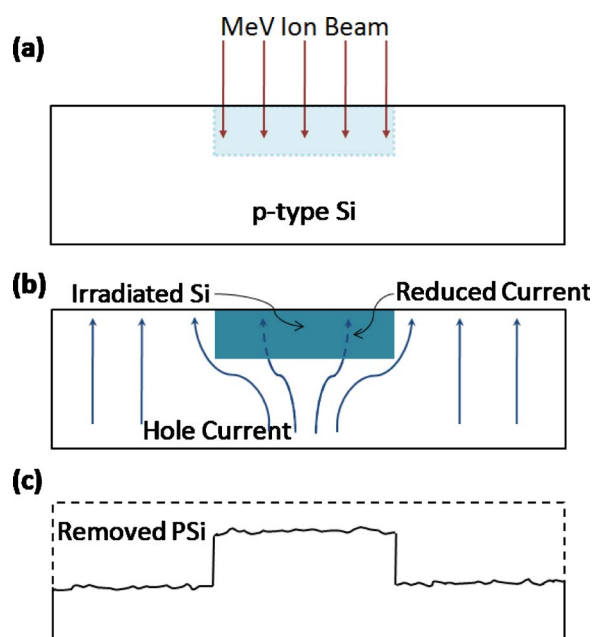


Figure 1. (Color online) Schematic of the effect of ion irradiation of a well-defined region. (a) Ion irradiation, (b) electrochemical anodization, and (c) porous silicon removal.

<sup>z</sup> E-mail: g0800837@nus.edu.sg

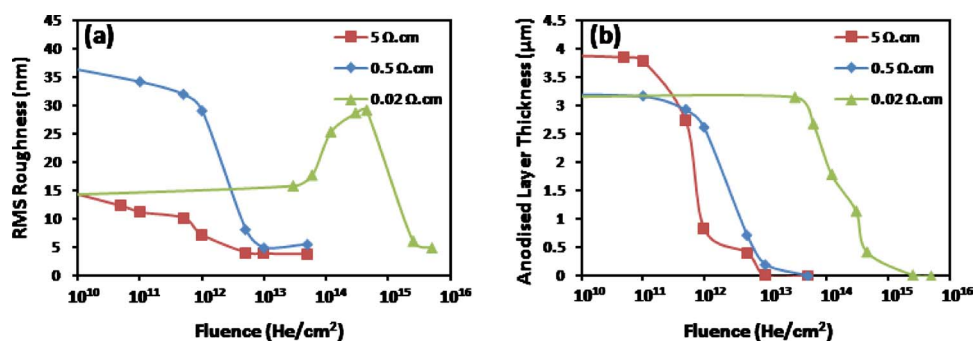


Figure 2. (Color online) (a) Surface roughness vs helium ion fluence for three wafer resistivities, anodized using a current density of  $50 \text{ mA}/\text{cm}^2$ . (b) Anodized depth vs helium ion fluence for three wafer resistivities.

and unetched regions and was measured using a profilometer after PSi removal. A thinner porous silicon layer consequently forms at the irradiated area (Fig. 1c) and the roughness of the exposed irradiated and unirradiated silicon surfaces is measured using an atomic force microscope.

The aim of this study is to determine whether the more deeply anodized, unirradiated surface or the irradiated surface anodized with a lower current density is rougher. Figure 2 shows the measured surface roughness and anodized layer thickness of the irradiated areas of  $1 \text{ mm}^2$  as a function of 1 MeV helium ion (range  $3.5 \mu\text{m}$  in silicon) fluence for the three wafer resistivities. Ion irradiation reduces the current density and slows down the rate of anodization in each case, as shown in Fig. 2b. However, Fig. 2a exhibits a more subtle dependence of the resultant surface roughness of the irradiated areas on the fluence. For the moderate resistivity wafers, the roughness decreases with fluence, consistent with the anodized layer thickness being the dominant factor.<sup>13</sup> However, for the low resistivity wafer, the roughness increases with fluence, so even though the anodized layer is thinner at the irradiated regions, it has a rougher surface compared with the thicker, unirradiated background. At high fluences, the roughness drops sharply simply because the anodization rate is reduced to almost zero.

Although rather counterintuitive, the observation of increasing roughness with fluence for the low resistivity wafer can be explained by considering the change in resistivity within the irradiated regions due to increasing ion fluence, as shown in Fig. 3. The defect distribution produced by 2 MeV helium ions was calculated using the code Stopping and Range of Ions in Matter,<sup>14</sup> and the effect of each defect on the reduced carrier density is described in Ref. 1. Three zones of resistivity of p-type silicon are indicated, whereby mesoporous, microporous, or macroporous silicon tends to form during anodization.<sup>7</sup> The horizontally running arrows show the range of

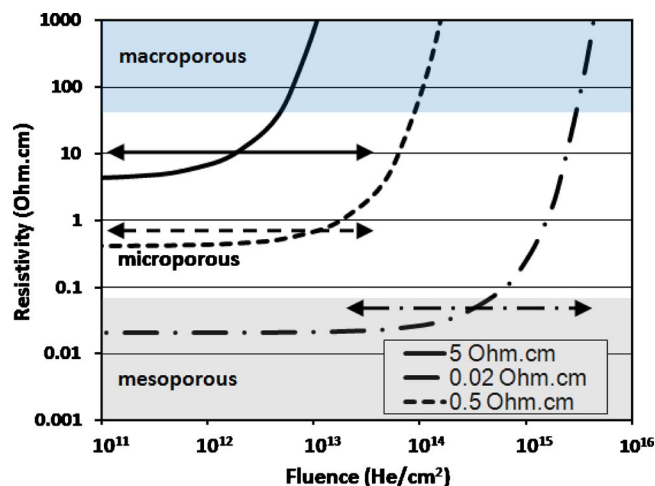


Figure 3. (Color online) Calculated change in resistivity vs MeV helium ion fluence for wafer resistivities of 0.02, 0.5, and  $5 \Omega \cdot \text{cm}$ .

fluences over which variations in roughness and anodization rate are observed in Fig. 2. The irradiation of the moderate resistivity wafers ( $0.5$  and  $5 \Omega \cdot \text{cm}$ ) results in the increased resistivity of the irradiated regions still lying within the range for which microporous silicon tends to be produced. However, the irradiation of the low resistivity ( $0.02 \Omega \cdot \text{cm}$ ) wafer results in the resistivity increasing from the regime where mesoporous silicon tends to form into the more resistive region in which microporous silicon tends to form, with its associated high roughness. Hence, for low wafer resistivities, the increased resistivity of the irradiated regions is the dominant factor determining the surface roughness, rather than the anodized layer thickness.

To confirm this hypothesis for the increased resistivity of low resistivity wafers strongly modifying their anodization behavior and the properties of the resultant PSi, Fig. 4 shows previously published data for the variation in PL intensity for the  $0.02 \Omega \cdot \text{cm}$  wafer as a function of helium ion fluence. For this purpose, the PSi removal stage in Fig. 1c is left out. A strong increase in PL intensity is observed at fluences of  $10^{13}$ – $10^{15}/\text{cm}^2$ , similar to the range of fluences over which the surface roughness increases. This is compatible with our hypothesis, because mesoporous silicon produced during anodization of low resistivity wafers does not produce intense PL owing to a low density of nanometer-size silicon crystallites which emit PL by quantum confinement. In comparison, intense PL is produced by microporous silicon which has a high density of nanometer-size silicon crystallites, so as the resistivity of the irradiated areas rises, so does the PL emission as more microporous silicon is formed, even though the anodized layer becomes thinner.

This result is important in understanding the basic mechanisms and effects of ion irradiation of p-type wafers and defines the different behaviors of surface roughness and PL intensity that can occur. Modified resistivity is an important aspect in determining the properties of the resultant anodized porous silicon and underlying silicon surface, which is an important understanding for this process of silicon micromachining.

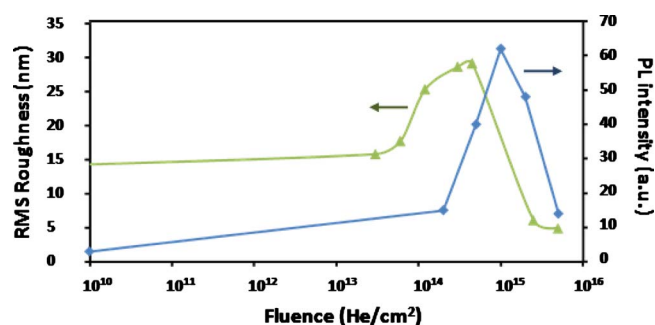


Figure 4. (Color online) Variation in PL intensity vs helium ion fluence for  $0.02 \Omega \cdot \text{cm}$  wafer resistivity; data reproduced from Ref. 6. Roughness data for the same material from Fig. 2a are overlaid for comparison.

### Acknowledgment

The authors acknowledge the financial support from the MOE Academic Research Fund under grant no. R144 000 238 112.

*National University of Singapore assisted in meeting the publication costs of this article.*

### References

1. M. B. H. Breese, F. J. T. Champeaux, E. J. Teo, A. A. Bettiol, and D. J. Blackwood, *Phys. Rev. B*, **73**, 035428 (2006).
2. I. Rajta, S. Z. Szilasi, P. Fürjes, Z. Fekete, and C. Dúcsó, *Nucl. Instrum. Methods Phys. Res. B*, **267**, 2292 (2009).
3. P. Polesello, C. Manfredotti, F. Fizzotti, R. Lu, E. Vittone, G. Lerondel, A. M. Rossi, G. Amato, L. Boarino, S. Galassini, et al., *Nucl. Instrum. Methods Phys. Res. B*, **158**, 173 (1999).
4. F. Menzel, D. Spemann, J. Lenzner, W. Böhlmann, G. Zimmermann, and T. Butz, *Nucl. Instrum. Methods Phys. Res. B*, **267**, 2321 (2009).
5. F. Nespriás, M. Venturino, M. E. Debray, J. Davidson, M. Davidson, A. J. Kreiner, D. Minsky, M. Fischer, and A. Lamagna, *Nucl. Instrum. Methods Phys. Res. B*, **267**, 69 (2009).
6. E. J. Teo, M. B. H. Breese, A. A. Bettiol, D. Mangaiyarkarasi, F. Champeaux, F. Watt, and D. J. Blackwood, *Adv. Mater.*, **18**, 51 (2006).
7. V. Lehmann, *Electrochemistry of Silicon: Instrumentation, Science, Materials and Applications*, Wiley-VCH, Weinheim, Germany (2002).
8. D. Mangaiyarkarasi, M. B. H. Breese, Y. S. Ow, and C. Vijila, *Appl. Phys. Lett.*, **89**, 021910 (2006).
9. H. F. Arrand, T. M. Benson, P. Sewell, and A. Loni, *J. Lumin.*, **80**, 199 (1998).
10. E. J. Teo, D. Mangaiyarkarasi, M. B. H. Breese, A. A. Bettiol, and D. J. Blackwood, *Appl. Phys. Lett.*, **85**, 4370 (2004).
11. K. Sugano and O. Tabata, *J. Micromech. Microeng.*, **12**, 911 (2002).
12. Y. S. Ow, S. Azimi, M. B. H. Breese, E. J. Teo, and D. Mangaiyarkarasi, *J. Vac. Sci. Technol. B*, **28**, 500 (2010).
13. G. Léronel, R. Romestain, and S. Barret, *J. Appl. Phys.*, **81**, 6171 (1997).
14. J. F. Ziegler, *Nucl. Instrum. Methods Phys. Res. B*, **219–220**, 1027 (2004).